

# Preliminary Investigation of Electromagnetic Thrust Characteristics in Electrodeless Compact Helicon Plasma Thruster

By Takahiro NAKAMURA<sup>1)</sup>, Hiroyuki NISHIDA<sup>1)</sup>, Shunjiro SHINOHARA<sup>1)</sup>, Ikkoh FUNAKI<sup>2)</sup>,  
Takao TANIKAWA<sup>3)</sup> and Tohru HADA<sup>4)</sup>

<sup>1)</sup>Department of Mechanical Systems Engineering, Tokyo University of Agriculture and Technology, Koganei, Japan

<sup>2)</sup>Institute of Space and Astronautical Science, JAXA, Sagami, Japan

<sup>3)</sup>Research Institute of Science and Technology, Tokai University, Hiratsuka, Japan

<sup>4)</sup>Interdisciplinary Graduate School of Engineering Sciences, Kyushu University, Kasuga, Japan

(Received June 28th, 2013)

In order to realize long-lived electric propulsion systems, we have been investigating an electrodeless plasma thruster. In our concept, high-density plasma from a compact helicon plasma source is accelerated by a magnetic nozzle for the thrust production. In order to optimize the thruster design, investigation of the thrust characteristics is needed. In this study, development of the electromagnetic thrust measurement system for compact helicon plasma thrusters and preliminary experiment of thrust measurement have been conducted. We have successfully developed a torsion-pendulum type thrust stand with measurement resolution of 10  $\mu\text{N}$ . From the thrust measurement, the electromagnetic thrust increases with the Ar gas mass flow rate and plasma production power. The thrust force and the electron density jump are observed due to the discharge mode transition from the inductively coupled plasma to the helicon wave excited plasma. The electromagnetic thrust force is up to 340  $\mu\text{N}$  (Ar gas mass flow rate of 1.0 mg/s, plasma production power of 400 W).

**Key Words:** Electrodeless Plasma Thruster, Thrust Measurement, Helicon Plasma

## Nomenclature

$\mathbf{B}$	: magnetic flux density vector
$F$	: thrust force
$J$	: electric current
$P$	: RF power
$\dot{m}$	: propellant mass flow rate
$n$	: number density
$r$	: radial distance
$T$	: temperature
$t$	: time
$z$	: axial distance
$\delta$	: displacement

## Subscripts

$e$	: electron
$EM$	: electromagnetic
$th$	: thermal
$r, z, \theta$	: component

## 1. Introduction

A helicon plasma source is one of the electrodeless plasma production methods using static magnetic field and radio frequency (RF) power, and can provide a high-density plasma in various size scales with high efficiency<sup>1)</sup>. Therefore, the helicon plasma source is expected to be applied for various sized electric propulsion system. Several types of the electrodeless plasma thrusters utilizing the helicon plasma source have been under development worldwide {e.g.

Variable Specific Impulse Magnetoplasma Rocket (VASIMR) (~200 kW, ~5.8 N)<sup>2-4)</sup>, Helicon Double Layer Thruster (HDLT) (~1 kW, 11mN)<sup>5-7)</sup>, Mini-helicon Plasma Thruster (~1 kW, ~10 mN)<sup>8)</sup>. In these concepts, the high density plasma is accelerated by divergent magnetic field (magnetic nozzle) for thrust production, and in the whole thrust production process, the electrodes do not contact with the plasma directly. This electrodeless configuration is one of promising solutions for the problems of the erosions and contaminations in conventional electric propulsion systems<sup>9)</sup>

Plasma acceleration by the magnetic nozzle has been investigated theoretically by Fruchtman in quasi-1-D model<sup>10)</sup>, and numerically by Ahedo and Merino in 2-D computation<sup>11)</sup>. These studies report that the detail plasmadynamics and the thrust production mechanism by the magnetic nozzle. Takahashi et al separately measured the electromagnetic thrust force and the thermal thrust force produced by the magnetic nozzle, and confirmed the magnetic nozzle theory<sup>12-15)</sup>. The previous researches indicated that the plasma pressure (electron pressure) has to be increased for higher thrust force, and stronger magnetic field is needed to confine higher plasma pressure. In addition, stronger magnetic field is needed to achieve the actual thrust force close to the theoretical limit in the experiment. The research group of the VASIMR showed high input power (up to 200 kW) and strong magnetic field (up to 2 T) could provide high performance. However, high input power and strong magnetic field leads to the requirement of large facility and complicated system such as high-power electric supply and superconducting coil.

In order to achieve high performance with moderate-size

thruster and simple system (moderate strength of magnetic field), we have proposed electrodeless electromagnetic plasma acceleration by additional RF power input in addition to the magnetic nozzle. Combination of a helicon plasma source, the magnetic nozzle and the additional electromagnetic plasma acceleration is expected to realize the high performance compact plasma thruster<sup>16)</sup>.

In order to develop electrodeless electromagnetic plasma acceleration technique by the RF power input, we have initiated the HEAT (Helicon Electrodeless Advanced Thruster) project in Japan, and have been investigating various type (thruster size, power and plasma acceleration method) electrodeless propulsion systems utilizing a helicon plasma source<sup>17)</sup>.

In our concept (as shown in Fig. 1), the high density helicon plasma passing through the magnetic nozzle is electromagnetically accelerated by additional RF rotating electric field (REF) power input<sup>18,19)</sup>. The entire process can be conducted without contacts between electrodes and the plasma by using RF antennas outside of the discharge chamber. In this concept, as a first stage of the thrust force generation, the helicon plasma is accelerated and exhausted by passed through the magnetic nozzle. In this stage, the Lorentz force, which is product of the diamagnetic current and diverging magnetic field, turns into the electromagnetic thrust force (Fig. 2,  $F_{diamag}$ ). In addition, the thermal pressure of the plasma, which acts on the thruster end plate, turns into the thermal thrust (Fig. 2,  $F_{th}$ ). As a next stage, in order to enhance the electromagnetic thrust force, an azimuthal electric current is induced by the additional REF power, and the plasma is electromagnetically accelerated in the magnetic nozzle (Fig. 2,  $F_{accel}$ ).

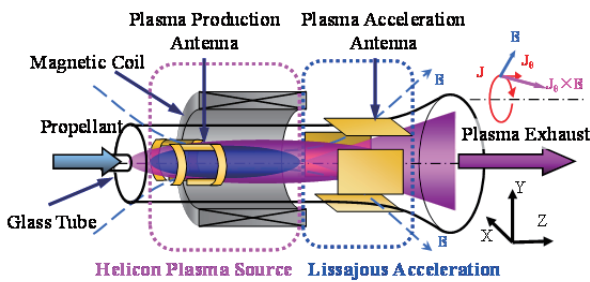


Fig. 1. Concept of Lissajous acceleration type plasma thruster.

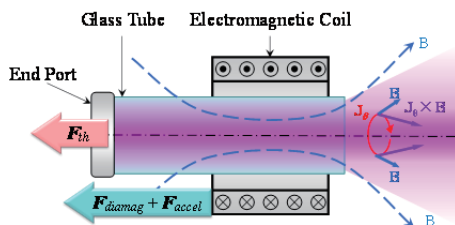


Fig. 2. Electromagnetic thrust force and thermal thrust force acting on the thruster components.

We have developed and investigated the compact sized laboratory model of the REF-type helicon plasma thruster<sup>20-22)</sup>. Our laboratory model has simple and compact magnetic

circuit constructed by permanent magnets which are located in the single annular layer; this is more compact and light-weight structure than the other magnetic circuit using permanent magnets<sup>13, 24)</sup>. In our previous studies, high density helicon plasma was successfully produced with this configuration<sup>23)</sup>.

Before investigation the additional REF plasma acceleration, the thrust characteristics of the simple helicon plasma thruster (only with the magnetic nozzle and without REF acceleration) and plasma parameter of the plume have to be identified in detail. In this study, we develop a high resolution electromagnetic thrust force measurement system which can measure several tens micro Newton, and thrust measurement of a simple compact helicon plasma thruster (without REF acceleration) is conducted. In addition to the thrust measurement, the plasma parameters (electron density and electron temperature) are measured using an electrostatic double probe.

## 2. Measurement Setup

A torsion-pendulum type thrust stand and a compact helicon plasma source are developed for the direct thrust measurement. The experimental setup is shown in Fig. 3. The thrust stand is installed within the vacuum chamber (I.D. 700 mm, 1200 mm long). The vacuum pumps (DRP 360II x3, ESV-10 x1) evacuate the chamber down to  $10^{-3}$  Pa or lower, and the Ar gas is fed as a propellant by mass flow controller at a predetermined mass flow rate.

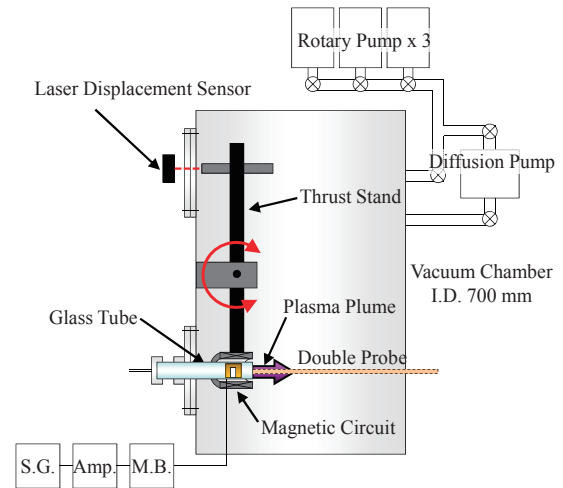


Fig. 3. Experimental facilities.

A schematic of the laboratory model thruster is shown in Fig. 4. The thruster consists of a glass tube, a magnetic circuit, a plasma production antenna and plasma acceleration antennas. A 26 mm I.D., totally 300 mm long glass tube is connected to a vacuum chamber (as shown in Fig.3). A double saddle type antenna (40 mm long) is used for the plasma production. The RF signal by a signal generator (Hewlett-Packard, 8648B) is amplified by a RF amplifier (Thamway, T145-5768A), and is transmitted to the antenna through a matching box (Thamway, T020-5558A). Here, the RF signal frequency for the plasma production is 27.12 MHz. The setup of the RF feeder is little

different from the previous experimental setup<sup>25</sup>). The RF antenna and coaxial cable are covered by the PTFE and grounded shield in order to suppress the plasma generation at the outside of the discharge chamber.

In order to measure the thrust force using a simple facility, only the magnetic circuit is mounted on the thrust stand and is mechanically isolated from the other thruster components. The plasma is accelerated by the Lorentz force when the plasma passed through the magnetic nozzle, and its reaction force acts on the magnetic circuit (When the additional REF power is applied, the reaction force from the REF electromagnetic plasma acceleration also acts on the magnetic circuit). Therefore, the thrust stand can measure the electromagnetic thrust force.

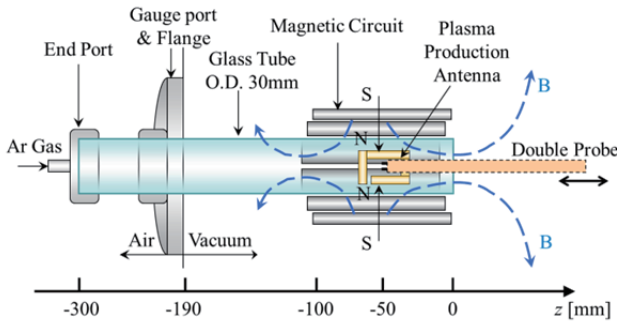


Fig. 4. Schematic of laboratory model thruster configuration.

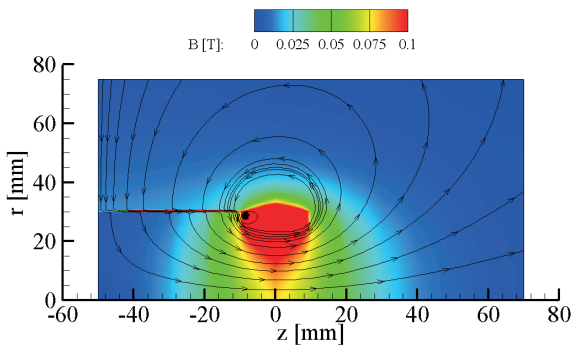


Fig. 5. Magnetic field distribution in  $r-z$  plane.

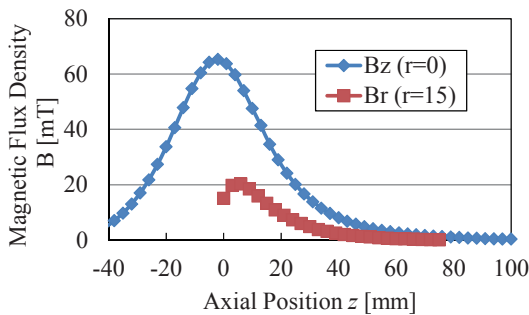


Fig. 6. Axial profiles of magnetic flux density  $B_z$  ( $r = 0$  mm) and  $B_r$  ( $r = 15$  mm).

The magnetic circuit is constructed using 22 samarium-cobalt magnets, which are arranged in an annular

shape (I.D. 50 mm). The magnetic north pole of all magnets is directed to the inside of the thruster. The magnetic flux density profiles are shown in Figs. 5 and 6; this magnetic flux density is enough for the helicon plasma discharge.

The electromagnetic force acting on the magnetic circuit results in a displacement of the pendulum arm. This arm displacement is measured by a laser displacement sensor (KEYENCE, LK-G35A), which has an accuracy of 0.5  $\mu$ m. Two hinges (SDP/SI, SS99FXS018720) are used as a pivot of the pendulum (Fig.7). A damping force is applied to the pendulum arm by the magnetic dumper, which consists of a permanent magnet near the pendulum arm.

The relation between the thrust force and displacement is calibrated by applying repelling force using a samarium-cobalt bar magnet (4 mm diameter, 27 mm long) and an electromagnetic coil (7.15 mm diameter, 16.25 mm long, 13 turn) which are installed at 59.5 mm from the pivot (Fig. 8). The repelling force is measured by the electric balance (SHIMADZU, LIBROR AEX-200B), which has an accuracy of 0.1 mg (Fig. 9). The relation between coil current and repelling force is shown in Fig. 10. A main factor of the error in this repelling force comes from a positioning accuracy between the bar magnet and the electromagnetic coil. The error in the repelling force is evaluated within  $\pm 6.5$   $\mu$ N by the standard deviation of 10 times measurement. The equivalent thrust force is calculated from the repelling force divided by the arm ratio of 4.99. The sensitivity of the thrust stand is shown in Fig. 9 with straight line fitting. From this calibration, the sensitivity is found to be 2.3  $\mu$ N/ $\mu$ m. The error in the thrust sensitivity is evaluated as  $\pm 4.9$   $\mu$ N which is from the summation of the calibration unit accuracy ( $1.3$   $\mu$ N =  $6.5$   $\mu$ N / 4.99), an uncertainty of the laser displacement sensor ( $1.1$   $\mu$ N =  $2.3$   $\mu$ N/ $\mu$ m  $\times$   $0.5$   $\mu$ m) and the repetitive accuracy of the thrust stand ( $2.5$   $\mu$ N from the standard deviation of 5 times measurement). (Fig. 11).

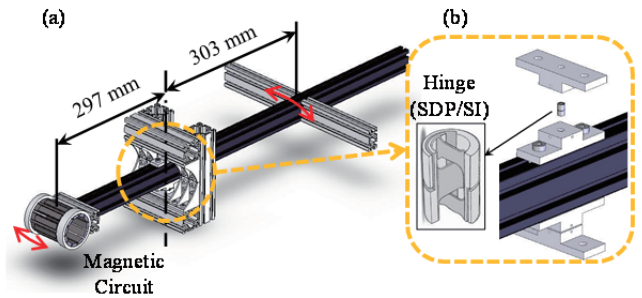


Fig. 7. (a) Torsion-pendulum type thrust stand, (b) Flexi-hinge.

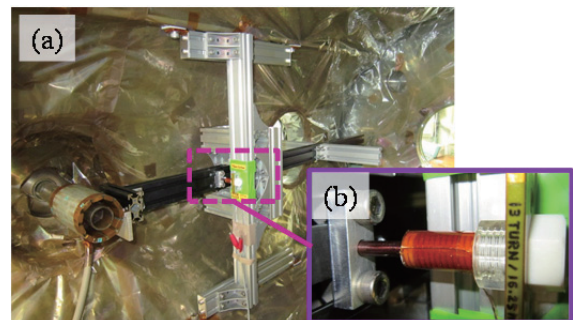


Fig. 8. (a) Thrust stand inside the vacuum chamber, (b) calibration unit.

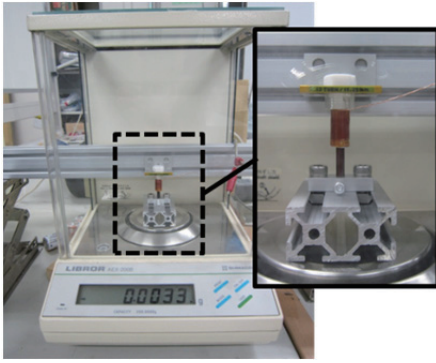


Fig. 9. Repelling force calibration by the electric balance.

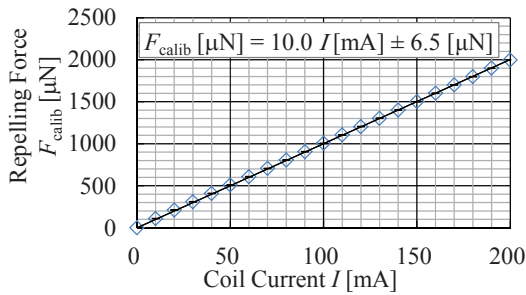


Fig. 10. Relation between coil current and repelling force.

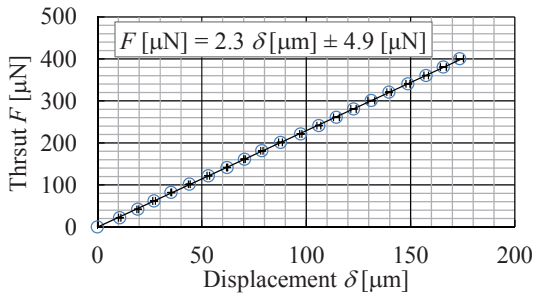


Fig. 11. Thrust stand sensitivity.

In addition to the thrust measurement, the plasma parameters (electron density and electron temperature) are measured using an electrostatic double probe (plasma collection area is 6.5 mm<sup>2</sup> × 2). The double probe is inserted to the thruster from an opposite chamber flange and measures the plasma parameters in the center of the plasma production antenna.

### 3. Experimental Results

Preliminary investigation of the thrust characteristics of compact helicon plasma source is conducted using our thrust measurement system. Experimental conditions are shown in Table 1.

Table 1. Experimental conditions.

Vacuum Pressure	$3.6 \times 10^{-2} \sim 1.6 \times 10^{-1}$ Pa
Ar Gas Mass Flow Rate	0.2, 0.4, 0.6, 0.8, 1.0 mg/s
Plasma Production Frequency	27.12 MHz
Plasma Production Power	100 ~ 400 W

The measurement starts under the condition without the RF power input to calibrate the zero position, and the RF power is turned-on 30 s later and power is kept constant for 30 s. The data are taken until 30 s after turned-off the RF power. Fig. 12 shows a typical result of the time history of the pendulum displacement. The pendulum swings when the RF power is turned-on and comes back to the zero position after the RF power is turned-off. The thrust force is evaluated from the difference between the mean values of the displacement with the RF power ( $t = 30$  to 60 s in Fig. 12) and without the RF power. In the case of Fig. 10, the thrust force is evaluated as 340 μN.

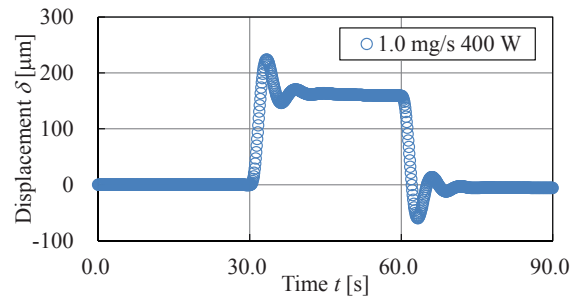


Fig. 12. Time history of pendulum displacement (experimental condition II, plasma production power of 400 W with a RF frequency of 27.12 MHz is turned-on from  $t = 30$  to 60 s, and Ar gas mass flow rate of 1.0 mg/s).

Figure 13 shows a relation between the measured electromagnetic thrust force and the plasma production power for various Ar gas mass flow rates. Error bars in the Fig. 13 are estimated from the standard deviation of 5 times measurement. The plasma production power  $P_{source}$  is defined as a subtraction of the forward RF power and the reflection RF power. The forward power and reflection power are obtained from directional coupler at the matching box. The thrust increases with the plasma production power and is up to 340 μN at 400 W with a mass flow rate of 1.0 mg/s. The electromagnetic thrust force abruptly increases around the plasma production power of 300 W. Figs. 14 and 15 plot the electron temperature and electron density measured at the center of the plasma production area, respectively. The density jump can be observed around the plasma production power of 300 W in Fig. 15. This thrust and density jump may be caused by the so-called density jump, which is a typical feature of the discharge mode transition from the inductively coupled plasma to the helicon wave excited plasma. From this experiment, the laboratory model thruster is found to generate the thrust force of sub-milli-newton even without the additional RF power. In this result, the electromagnetic thrust is higher (in the case of high Ar gas mass flow rate cases) or lower (in the case of low Ar gas mass flow rate cases) than the previous experimental results<sup>23)</sup>. It is considered that this difference of the electromagnetic thrust force comes from the RF feeder conditions. When the mass flow rate is relatively high, suppression of the plasma generation at the outside of the discharge chamber leads

reduction of the RF power loss at around the RF antenna, and helicon plasma is efficiently produced in the center of the discharge chamber. On the other hand, in the low mass flow rate case, the amount of the plasma reduces by suppressing the outside plasma generation.

This basic electromagnetic thrust force is lower than the other helicon plasma sources<sup>12-15, 24</sup>. The dimensions of our helicon plasma source are smaller diameter and longer length than the other helicon plasma sources. It is considered that the plasma loss on the discharge chamber wall leads lower thrust performance. In addition, magnetic field distribution and strength are not optimized for the thrust generation. The thrust performance is expected to be improved by the optimization of the thruster configuration (i.e. magnetic field distribution, Aspect ratio of the discharge chamber).

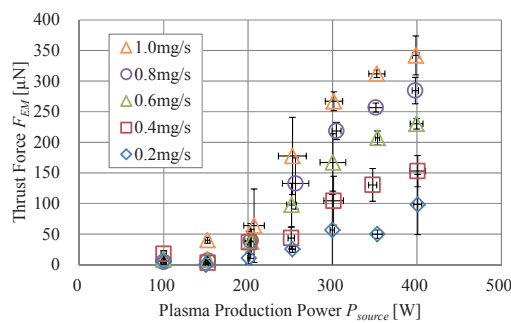


Fig. 13. Directly measured electromagnetic thrust as a function of plasma production power, changing Ar gas mass flow rate.

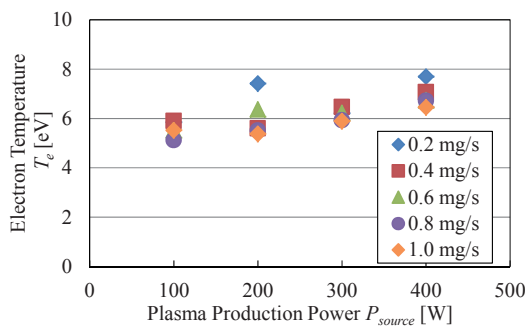


Fig. 14. Electron temperature measured by an electrostatic double probe in the center of the plasma production area ( $z = -50$  mm).

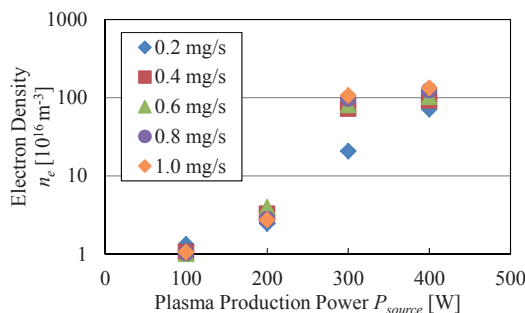


Fig. 15. Electron density measured by an electrostatic double probe in the center of the plasma production area ( $z = -50$  mm).

#### 4. Conclusions

In order to develop a long-life electric propulsion system, we have been investigating the electrodeless electromagnetic plasma thruster concept, utilizing a compact helicon plasma source and the Lissajous plasma acceleration. In order to evaluate the basic thrust performance of the compact helicon plasma source, torsion-pendulum type thrust stand system was developed, and the preliminary measurement of the electromagnetic thruster force acting on the magnetic circuit was conducted. We have successfully developed a torsion-pendulum type thrust stand with measurement resolution of 10  $\mu$ N. The electromagnetic thrust force increases with the plasma production power up to 340  $\mu$ N (plasma production power of 400 W, Ar gas mass flow rate of 1.0 mg/s). The thrust force and the density jump are observed at a plasma production power of 300 W due to the discharge mode transition from the inductively coupled plasma to the helicon wave excited plasma.

#### Acknowledgments

This work was supported by the Grants-in-Aid for Scientific Research under Contract No. (S) 21226019 from the Japan Society for the Promotion of Science.

#### References

- 1) Shinohara, S., Hada, T., Motomura, T., Tanaka, K., Tanikawa, T., et al.: Development of High-density Helicon Plasma Sources and Their Applications, *Phys. Plasmas*, **16** (2009), 057104.
- 2) Squire, J. P., Cassady, L. D., Chang Diaz, F. R., Carter, M. D., Glover, T. G., et al.: Superconducting 200 kW VASIMR Experiment and Integrated Testing, 31st Int. Electric Propul. Conf., IEPC-2009-209, 2009.
- 3) Cassady, L. D., Longmier, B. W., Olsen, C. S., Ballenger, M. G., McCaskill, G. E., et al.: VASIMR® Performance Results, 46th AIAA/ASME/SAE/ASEE Joint Propul. Conf. & Exhibit, AA-2010-6772, 2010.
- 4) Squire, J.P., Olsen, C. S., Franklin, R., Diaz, C., Cassedy, L. D., et al.: VASIMR® VX-200 Operation at 200kW and Plume Measurement: Future Plans and ISS EP Test Platform, 32nd Int. Electric Propul. Conf., IEPC-2011-154, 2011.
- 5) West, M. D., Charles C. and Boswell, R. W.: Testing a Helicon Double Layer Thruster Immersed in a Space-simulation Chamber, *J. Propul. Power*, **24** (2003), pp. 134-141.
- 6) Charles, C., Alexander, P., Costa, C., Sutherland, O., Boswell, R. W., et al.: Helicon Double Layer Thrusters, 29th Int. Electric Propul. Conf., IEPC-2005-290, 2005.
- 7) Musso, I., Manente, M., Carlsson, J., Giacomuzzo, C., Pavarin, D., et al.: 2D OOPIC Simulations of the Helicon Double Layer, 30th Int. Electric Propul. Conf., IEPC-2007-146, 2007.
- 8) Batishchev, O. V.: Minihelicon Plasma Thruster, *IEEE Trans. Plasma Sci.*, **10** (2009), 1563.
- 9) Toki, K., Shinohara, S., Tanikawa, T., Funaki, I. and Shamrai, K. P.: Preliminary Investigation of Helicon Plasma Source for Electric Propulsion Applications, 28th Int. Electric Propul. Conf., IEPC 03-0168, 2003.
- 10) Fruchtman, A.: Electric Field in a Double Layer and the Imparted Momentum, *Phys. Rev. Lett.*, **96** (2006), 065002.
- 11) Ahedo, E. and Merino, M.: Two-dimensional Supersonic Plasma Acceleration in a Magnetic Nozzle, *Phys. Plasmas*, **17** (2010), 073501.

- 12) Takahashi, K., Lafleur, T., Charles, C., Alexander, P., Boswell, R. W., et al.: Direct Thrust Measurement of a Permanent Magnet Helicon Double Layer Thruster, *Appl. Phys. Lett.*, **98** (2011), 141503.
- 13) Takahashi, K., Lafleur, T., Charles, C., Alexander, P. and Boswell, R. W.: Electron Diamagnetic Effect on Axial Force in an Expanding Plasma: Experiments and Theory, *Phys. Rev. Lett.*, **107** (2011), 235001.
- 14) Charles, C., Takahashi, K. and Boswell, R. B.: Axial force imparted by a conical radiofrequency magneto-plasma thruster, *Appl. Phys. Lett.*, **100** (2012), 113504.
- 15) Takahashi, K., Charles, C. and Boswell, R. W.: Approaching the Theoretical Limit of Diamagnetic-Induced Momentum in a Rapidly Diverging Magnetic Nozzle, *Phys. Rev. Lett.*, **110** (2013), 195003.
- 16) Toki, K., Shinohara, S., Tanikawa, T., Hada, T., Funaki, I., et al.: A Compact Helicon Source Plasma Acceleration by RF Antennae, JAXA Research and Development Report, JAXA-RR-09-003, 2010.
- 17) Shinohara, S., Nishida, H., Yokoi, K., Nakamura, T., Tanikawa, T., et al.: Research and Development of Electrodeless Plasma Thrusters Using High-Density Helicon Sources: The Heat Project, 32nd Int. Electric Propul. Conf., IEPC-2011-056, 2011.
- 18) Matsuoka, T., Funaki, I., Nakamura, T., Yokoi, K., Nishida, H., et al.: Scaling Laws of Lissajous Acceleration for Electrodeless Helicon Plasma Thruster, *Plasma Fus. Res.*, **6** (2011), 2406103.
- 19) Satoh, S., Matsuoka, T., Fujino, T. and Funaki, I.: A Theoretical Analysis for Electrodeless Lissajous Acceleration of HELICON Plasmas, 42th AIAA Plasmadynamics and Lasers Conf., AIAA-2011-4008, 2011.
- 20) Toki, K., Shinohara, S., Tanikawa, T., Funaki, I. and Shamrai, K. P.: Feasibility Study of Electrodeless Magnetoplasmadynamic Acceleration, 40th AIAA/ASME/SAE/ASEE Joint Propul. Conf. & Exhibit, AIAA-2004-3935, 2004.
- 21) Nakamura, T., Yokoi, K., Nishida, H., Matsuoka, T., Funaki, I., Shinohara, S., et al.: Study on Helicon Plasma Lissajous Acceleration for Electrodeless Electric Propulsion, *Trans. of JSASS Aerospace Tech. Japan*, **10** (2012), pp. Tb\_17-Tb\_23.
- 22) Nishida, H., Nakamura, T., Shinohara, S., Matsuoka, T., Funaki, I., et al.: Study on Proof-of-Principle of Lissajous Acceleration for Electrodeless Helicon Plasma Thruster, *Frontier of Appl. Plasma Tech.*, **5** (2012), pp. 67-72.
- 23) Takahashi, K., Nakamura, T., Nishida, H., Shinohara, S., Matsuoka, T., et al.: Study on Direct Measurement of Electromagnetic Thrust in Electrodeless Helicon Plasma Thruster, 13th Int. Space Conf. Pacific-basin Societies, AAS 12-520, 2012.
- 24) Matsuoka, T., Funaki, I., Satoh, S., Fujino, T., Iwabuchi, S., et al.: Laboratory Model Development of Lissajous Acceleration for Electrodeless Helicon Plasma Thruster, 48th AIAA/ASME/SAE/ASEE Joint Propul. Conf. & Exhibit, AIAA-2012-3956, 2012.
- 25) Nakamura, T., Takahashi, K., Nishida, H., Shinohara, S., Matsuoka, T., et al.: Direct Measurement of Electromagnetic Thrust of Electrodeless Helicon Plasma Thruster Using Magnetic Nozzle, *World Acad. Sci Eng. Tech.*, **71** (2012), pp. 797-801.